# On the Origin of High-Density Graphite Grains from the Murchison Meteorite

Sachiko Amari[a], Ernst Zinner[a] and Roberto Gallino[b]

[a]*McDonnell Center for the Space Sciences and the Physics Department, Washington University, One Brookings Drive, St. Louis, MO 63130, USA (sa@wuphys.wustl.edu).*
[b]*Dipartimento di Fisica Generale, Università di Torino, Via P. Giuria 1, I-10125 Torino, Italy.*

**Abstract.** The origin of high-density (2.10 – 2.20 g/cm$^3$) graphite grains from the Murchison meteorite is discussed. Distributions of the $^{12}C/^{13}C$ ratios of grains from the fractions KFB1 (2.10 –2.15 g/cm$^3$) and KFC1 (2.15 – 2.20 g/cm$^3$) are quite similar, having a pronounced peak around 400 – 630. From comparison with model calculations of asymptotic giant branch (AGB) stars we conclude that the grains in the peak most likely formed in low-mass (1.5, 2 and 3$M_\odot$) low-metallicity ($Z = 3 \times 10^{-3}$ for 1.5, 2 and 3$M_\odot$, $Z = 6 \times 10^{-3}$ for 3$M_\odot$ only) stars. s-Process Kr in KFC1 is best explained with 5$M_\odot$ stars of solar and/or half-solar metallicities.

**Keywords:** Presolar Grains; Dust; Meteorites; AGB stars, s-process.
PACS: 26.20.Fj; 26.20.Kn; 91.65.Dt; 96.30.Za; 97.20.Li.

## INTRODUCTION

Presolar grains are stardust found in primitive meteorites. These grains, which survived events during solar system formation and processes in meteorite parent bodies, retain information of their birthplace. The effort to decipher this information has established a new field of astronomy, laboratory analysis of presolar grains [1-3]. Mineral types of presolar grains identified to date include diamond [4], SiC [5, 6], graphite [7], refractory carbides [8], oxides [9-11] and silicates [12-15]. The abundances of these grains are only a few hundred ppm or less in bulk meteorites.

Graphite is one of the mineral types that carry isotopically anomalous noble gases [7]. Graphite grains extracted from the Murchison and Orgueil meteorites show a range of densities [16, 17]. From the Murchison meteorite, four graphite-rich fractions have been extracted: KE3 (1.65 – 1.72 g/cm$^3$), KFA1 (2.05 – 2.10 g/cm$^3$), KFB1 (2.10 – 2.15 g/cm$^3$) and KFC1 (2.15 – 2.20 g/cm$^3$) [16]. One of the most interesting and intriguing characteristics of graphite grains is that isotopic and elemental abundances depend on density.

Figure 1 shows C isotopic distributions of these fractions. All the fractions have a peak at the bin with $^{12}C/^{13}C$ ratios between 79 and 100. Since many grains in this bin have solar $^{12}C/^{13}C$ ratio (89), we interpret this to be due to the presence of solar system grains in addition to presolar grains. KE3 and KFA1 have a broad distribution. Many KE3 and KFA1 grains show $^{18}O$ excesses, $^{15}N$ excesses, high $^{26}Al/^{27}Al$ ratios, Si isotopic anomalies [18, 19]. These are the signatures of core-collapse supernovae, where different nucleosynthetic processes take place in different zones before the explosion [19]. Oxygen-18 excesses in many grains reflect alpha-capture on $^{14}N$ in the

He/C zone. High $^{26}Al/^{27}Al$ ratios are produced in the He/N zone via the $^{25}Mg(p,\gamma)$ reaction. Silicon isotopic anomalies, mainly $^{28}Si$ excesses, but also excesses in $^{29}Si$ and $^{30}Si$, indicate O-burning and neutron capture reactions, respectively. Evidence of the initial presence of $^{44}Ti$ in a few grains is a definite proof of a supernova origin because $^{44}Ti$ is produced only during explosive nucleosynthesis [19, 20].

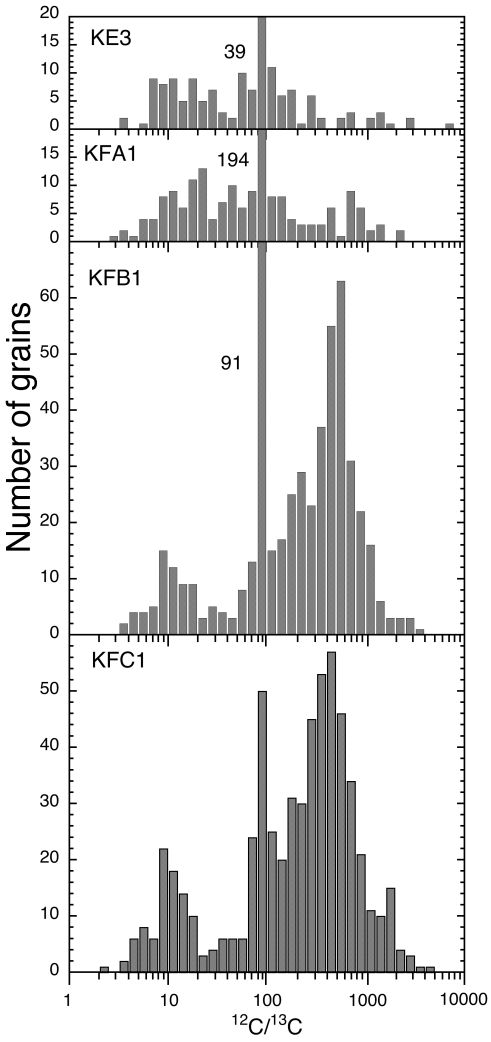


**FIGURE 1.** Carbon isotopic distributions of grains from the Murchison density fractions, KE3, KFA1, KFB1 and KFC1. The numbers in the figure indicates the numbers of the grains in the bins that exceed the scales [21].

KFB1 and KFC1 have two distinct peaks in their C isotopic distributions, one with the peak around 10, the other with the peak around 400 – 630 (500 – 630 for KFB1 and 400 – 500 for KFC1) (Fig. 1). The high $^{12}C/^{13}C$ ratios in the latter are consistent with a low-metallicity AGB star origin of the grains. Bulk noble gas analysis indicates that KFC1 grains originated in low-metallicity AGB stars ($Z \leq 0.002$) [22]. TEM studies of slices of KFC1 grains found subgrains that are highly enriched in s-process elements, confirming that KFC1 grains formed in low-metallicity AGB stars [23, 24].

Noble gas analyses of single KFB1 and KFC1 grains also provided evidence that some of the grains originated from low-metallicity AGB stars [25, 26].

In this study, we will compare the C isotopic data of single graphite grains and Kr data of bulk (=aggregate) samples from KFC1 as well as KFB1 with improved model calculations of AGB stars to further constrain the origin of these grains. We will focus on the grains belonging to the peak at higher than solar $^{12}C/^{13}C$ ratios. The origin of grains with low $^{12}C/^{13}C$ ratios ($\leq 20$) remains controversial and an AGB star origin can be excluded because of their low $^{12}C/^{13}C$ ratios.

## CARBON ISOTOPIC RATIOS

Table 1 summarizes the ranges of $^{12}C/^{13}C$ and the C/O of the C-rich envelope following the last thermal pulse obtained from AGB models for stars with various masses and metallicities. It is not likely that a single type of stars, with a specific mass and metallicity, formed the KFC1 grains. More likely is that stars with a range of mass and metallicity produced these grains. Since the peak at the C isotopic distribution is around 400 – 500 (Fig. 1), the $^{12}C/^{13}C$ ratios of the envelope should have reached ~ 500 or more at the end of the third dredge-up episode. The masses and metallicities of the stars that satisfy this condition are 1.5 $M_\odot$ $Z = 3 \times 10^{-3}$, 2 $M_\odot$ $Z = 3 \times 10^{-3}$, 3 $M_\odot$ $Z = 3 \times 10^{-3}$ and 3 $M_\odot$ $Z = 6 \times 10^{-3}$ (shown in italics in Table 1). They are low-mass (1.5 – 3 $M_\odot$) low-metallicity ($Z \leq 6 \times 10^{-3}$) stars. Particularly the 3 $M_\odot$ $Z = 3 \times 10^{-3}$ case can explain grains with high $^{12}C/^{13}C$ ratios (> 1000) observed in KFC1.

**TABLE 1.** Carbon isotopic ranges of the C-rich envelope and C/O ratios of the envelope at the last pulse for stars with various masses and metallicities [27].

| Mass ($M_\odot$) | Metallicity (Z) | Range of $^{12}C/^{13}C$ ratios of C-rich Envelope | C/O of Envelope after the Last Thermal Pulse |
|---|---|---|---|
| 1.5 | *$3 \times 10^{-3}$* | *67 – 761* | *12.5* |
| | $6 \times 10^{-3}$ | 54 – 239 | 4.94 |
| | $1 \times 10^{-2}$ | 44 – 90 | 2.13 |
| | $2 \times 10^{-2}$ | 38 – 43 | 1.16 |
| 2 | *$3 \times 10^{-3}$* | *68 – 1305* | *18.95* |
| | $6 \times 10^{-3}$ | 51 – 372 | 7.40 |
| | $1 \times 10^{-2}$ | 42 – 152 | 3.48 |
| | $2 \times 10^{-2}$ | 37 – 56 | 1.51 |
| 3 | *$3 \times 10^{-3}$* | *108 – 2521* | *16.72* |
| | *$6 \times 10^{-3}$* | *103 – 650* | *6.18* |
| | $1 \times 10^{-2}$ | 93 – 349 | 3.82 |
| | $2 \times 10^{-2}$ | 84 – 141 | 1.80 |
| 5 | $3 \times 10^{-3}$ | 108 – 360 | 3.15 |
| | $6 \times 10^{-3}$ | 99 – 240 | 2.40 |
| | $1 \times 10^{-2}$ | 89 – 169 | 1.87 |
| | $2 \times 10^{-2}$ | 80 – 108 | 1.36 |

## KRYPTON ISOTOPIC RATIOS

Krypton-86 yields are a sensitive indicator of nucleosynthetic conditions. There is an s-process branching point at $^{85}$Kr, which decays to $^{85}$Rb with the half-life of 11 years. Therefore, $^{86}$Kr/$^{82}$Kr ratios depend on neutron density. Amari et al. [22] analyzed noble gases in the Murchison graphite bulk samples and found that KFC1 contains s-process Kr with high $^{86}$Kr/$^{82}$Kr (Kr-SH), while s-process Kr with low $^{86}$Kr/$^{82}$Kr (Kr-SL) was dominant in the other density fractions. Here we will examine s-process Kr inferred from the graphite data and compare it with the pure s-process Kr produced in the He-shell, rather than examine the graphite data themselves and compare them with the Kr isotopic ratios in the envelope. The reason for this is that the Kr analysis was carried out on bulk samples, thus the released Kr originated not entirely from presolar graphite but also from solar system grains in the density fractions. Amari et al. [22] used 0.3 as the s-process $^{83}$Kr/$^{82}$Kr ratio to infer the s-process $^{86}$Kr/$^{82}$Kr ratio. This ratio has been updated to 0.375 [28]. Here we also use 0.375 as the s-process $^{83}$Kr/$^{82}$Kr and infer the s-process $^{86}$Kr/$^{82}$Kr to be 4.43 ± 0.46.

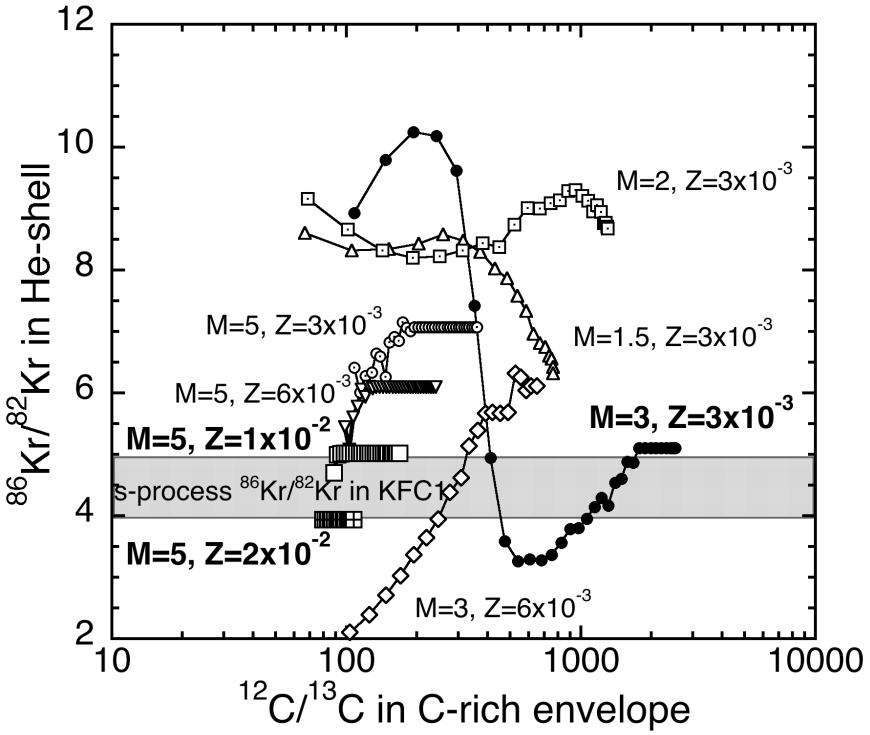


**FIGURE 2.** Model $^{86}$Kr/$^{82}$Kr ratios in the He-shell of AGB stars, when the envelope becomes C-rich, are plotted against the $^{12}$C/$^{13}$C ratios of the envelope. The s-process $^{86}$Kr/$^{82}$Kr in KFC1 [28] is shown as the shadowed box. The data for s-process Kr are from [29].

Figure 2 shows model $^{86}$Kr/$^{82}$Kr ratios in the He-shell and $^{12}$C/$^{13}$C ratios of the C-rich envelope for a series of thermal pulses. We only plot the cases where s-process $^{86}$Kr/$^{82}$Kr ratios equal or exceed 4 at the last thermal pulse. In the M = 1.5 $M_\odot$ Z = 3 × $10^{-3}$ and M = 2 $M_\odot$ Z = 3 × $10^{-3}$ cases, the $^{86}$Kr/$^{82}$Kr ratios are always higher than 5. For the M = 3$M_\odot$ Z = 6 × $10^{-3}$ case, the ratios are in the range of KFC1 Kr during a few pulses but they quickly increase to higher values for higher pulse numbers. For

the M = 3 $M_\odot$ Z = $3 \times 10^{-3}$ case, the ratio starts from above 10 and quickly goes down to 2, reaches at ~ 4 at the 19th pulse then gradually increases to 5.1. For M = $5M_\odot$, $^{86}Kr/^{82}Kr$ ratios for the two low-metallicity cases ($Z \leq 6 \times 10^{-3}$) are too high to account for the Kr in KFC1. Those of the two higher metallicity cases, Z = $1 \times 10^{-2}$ and Z = $2 \times 10^{-2}$, match the s-process $^{86}Kr/^{82}Kr$ in KFC1. However, these two cases cannot explain the whole C isotopic range of the peak of interest in KFC1 (see Table 1).

## STELLAR SOURCES OF KFC1 AND KFB1 GRAINS

From the C isotopic ratios and the s-process Kr in KFC1 grains, we have identified AGB stars with somewhat different ranges of masses and metallicities as stellar sources of KFC1 grains. From the former, low-mass (1.5, 2 and $3M_\odot$) and low-metallicity [Z = $3 \times 10^{-3}$ and Z = $6 \times 10^{-3}$ (for $3M_\odot$ only)] stars are likely sources. From the latter, slightly higher mass stars with a range of metallicity ($3M_\odot$ Z = $3 \times 10^{-3}$, $5M_\odot$ Z = $1 \times 10^{-2}$, $5M_\odot$ Z = $2 \times 10^{-2}$) are identified as sources. The only case that satisfies both the C and the Kr isotopic ratios is the M=$3_\odot$ Z = $3 \times 10^{-3}$ case and it is tempting to consider such stars as the stellar sources of the KFC1 grains.

However, we have to take KFB1 grains into account. These grains have a similar C isotopic distribution (Fig. 1) but a completely different s-process Kr with a much lower $^{86}Kr/^{82}Kr$ ratio (Kr-SL) [22]. If the M = $3M_\odot$ Z = $3 \times 10^{-3}$ case produced Kr-SH found in KFC1, it is hard to explain why KFB1, which has a similar C isotopic distribution, lacks Kr-SH. Therefore, we have to conclude that stars with M = $3M_\odot$ Z = $3 \times 10^{-3}$ are not a source of the Kr-SH. It might be because graphite grains had been already carried away far from the star when a substantial amount of Kr was dredged-up into the envelope. A closer inspection shows that there are more grains with $^{12}C/^{13}C$ ratios around ~ 100 in KFC1 than in KFB1 (see Fig. 1). In the M = $5M_\odot$ cases (Z = $1 \times 10^{-2}$ and $2 \times 10^{-2}$), C isotopic ratios ranges in the C-rich envelope are expected to range from 89 to 169 and from 80 to 108, respectively. Therefore, if these stars are sources of Kr-SH, the C and the Kr isotopic ratios of both KFC1 and KFB1 can be explained.

## CONCLUSIONS

Presolar graphite grains show a range of density and their isotopic features depend on density. In Murchison graphite grains, a significant portion of low-density grains, those from the fractions KE3 and KFA1, most likely formed in core-collapse supernovae. The carbon isotopic distribution of KFC1 shows two peaks, one at lower $^{12}C/^{13}C$ ratios than the solar ratio and the other around 400 –500. The high ratios are indicative of an origin in low-mass (1.5 – 3 $M_\odot$) low-metallicity ($Z \leq 6 \times 10^{-3}$) AGB stars. KFC1 contains an s-process Kr component that is characterized by a high $^{86}Kr/^{82}Kr$ ratio (4.43 ± 0.46) (Kr-SH). When KFB1, which has a C isotopic distribution similar to that of KFC1 but has a completely different s-process Kr, is taken into account, $5M_\odot$ stars of Z = $1 \times 10^{-2}$ and $2 \times 10^{-2}$ are likely sources of the Kr in KFC1.

## ACKNOWLEDGMENTS

This work was supported by NASA grants, NNX10AI45G, NNX11AH14G and NNX12AB24G. We thank the anonymous reviewer for constructive comments, which improved the manuscript.

## REFERENCES

1. T. J. Bernatowicz and E. Zinner, "*Astrophysical Implications of the Laboratory Study of Presolar Materials*", AIP Conf. Proc. **402**, AIP, New York, 1997, pp. 750.
2. K. Lodders and S. Amari, *Chem. Erde* **65**, 93-166 (2005).
3. E. Zinner "Presolar grains", in *Meteorites, Planets, and Comets*, edited by A. M. Davis, Vol. 1 Treatise on Geochemistry, edited by H. D. Holland and K. K. Turekian, edited by Elsevier-Pergamon, Oxford, 2004, pp. 17-39.
4. R. S. Lewis, M. Tang, J. F. Wacker, E. Anders and E. Steel, *Nature* **326**, 160-162 (1987).
5. T. Bernatowicz, G. Fraundorf, M. Tang, E. Anders, B. Wopenka, E. Zinner and P. Fraundorf, *Nature* **330**, 728-730 (1987).
6. M. Tang and E. Anders, *Geochim. Cosmochim. Acta* **52**, 1235-1244 (1988).
7. S. Amari, E. Anders, A. Virag and E. Zinner, *Nature* **345**, 238-240 (1990).
8. T. J. Bernatowicz, S. Amari, E. K. Zinner and R. S. Lewis, *Astrophys. J.* **373**, L73-L76 (1991).
9. I. D. Hutcheon, G. R. Huss, A. J. Fahey and G. J. Wasserburg, *Astrophys. J.* **425**, L97-L100 (1994).
10. G. R. Huss, A. J. Fahey, R. Gallino and G. J. Wasserburg, *Astrophys. J.* **430**, L81-L84 (1994).
11. L. R. Nittler, C. M. O'D. Alexander, X. Gao, R. M. Walker and E. K. Zinner, *Nature* **370**, 443-446 (1994).
12. S. Messenger, L. P. Keller, F. J. Stadermann, R. M. Walker and E. Zinner, *Science* **300**, 105-108 (2003).
13. A. N. Nguyen and E. Zinner, *Science* **303**, 1496-1499 (2004).
14. K. Nagashima, A. N. Krot and H. Yurimoto, *Nature* **428**, 921-924 (2004).
15. S. Mostefaoui and P. Hoppe, *Astrophys. J.* **613**, L149-L152 (2004).
16. S. Amari, R. S. Lewis and E. Anders, *Geochim. Cosmochim. Acta* **58**, 459-470 (1994).
17. M. Jadhav, S. Amari, K. K. Marhas, E. Zinner, T. Maruoka and R. Gallino, *Astrophys. J.* **682**, 1479-1485 (2008).
18. S. Amari, E. Zinner and R. S. Lewis, *Astrophys. J.* **447**, L147-L150 (1995).
19. C. Travaglio, R. Gallino, S. Amari, E. Zinner, S. Woosley and R. S. Lewis, *Astrophys. J.* **510**, 325-354 (1999).
20. F. X. Timmes, S. E. Woosley, D. H. Hartmann and R. D. Hoffman, *Astrophys. J.* **464**, 332-341 (1996).
21. S. Amari, E. Zinner and R. Gallino, *Astrophys. J.* submitted (2012).
22. S. Amari, R. S. Lewis and E. Anders, *Geochim. Cosmochim. Acta* **59**, 1411-1426 (1995).
23. T. J. Bernatowicz, R. Cowsik, P. C. Gibbons, K. Lodders, B. Fegley, Jr., S. Amari and R. S. Lewis, *Astrophys. J.* **472**, 760-782 (1996).
24. T. K. Croat, F. J. Stadermann and T. J. Bernatowicz, *Astrophys. J.* **631**, 976-987 (2005).
25. P. R. Heck, S. Amari, P. Hoppe, H. Baur, R. S. Lewis and R. Wieler, *Astrophys. J.* **701**, 1415-1425 (2009).
26. M. M. M. Meier, P. R. Heck, S. Amari, H. Baur and R. Wieler, *Geochem. Cosmochim. Acta* **76**, 147-160 (2012).
27. S. Bisterzo, R. Gallino, O. Straniero, S. Cristallo and F. Käppeler, *Mon. Not. R. Astron. Soc.* **404**, 1529-1544 (2010).
28. S. Amari, R. Gallino, M. Limongi and A. Chieffi "Presolar graphite from the Murchison meteorite: Imprint of nucleosynthesis and grain formation", in *Origin of Matter and Evolution of Galaxies: International Symposium on Origin of Matter and Evolution of Galaxies 2005: New Horizon of Nuclear Astrophysics and Cosmology*, edited by S. Kubono, W. Aoki, T. Kajino, T. Motobayashi and K. Nomoto, AIP, 2006, pp. 311-318.
29. S. Bisterzo and R. Gallino (private communication).